The Glass and Jamming transitions in dense granular matter

Corentin Coulais*, Raphaël Candelier† and Olivier Dauchot**

*SPHYNX/SPEC, CEA-Saclay, URA 2464 CNRS, 91 191 Gif-sur-Yvette, France
†UPMC Univ. Paris 06, FRE 3231, LJP, F-75005, Paris, France
**EC2M/UMR 7083 Gulliver, ESPCI-ParisTech, 75005 Paris, France

Abstract. Everyday life tells us that matter acquires rigidity either when it cools down, like lava flows which turn into solid rocks, or when it is compacted, like tablets simply formed by powder compression. As suggested by these examples, solidification is not the sole privilege of crystals but also happens for disordered media such as glass formers, granular media, foams, emulsions and colloidal suspensions. Fifteen years ago the "Jamming paradigm" emerged to encompass in a unique framework the glass transition and the emergence of yield stress, two challenging issues in modern condensed matter physics. One must realize how bold this proposal was, given that the glass transition is a finite temperature transition governing the dynamical properties of supercooled liquids, while Jamming is essentially a zero temperature, zero external stress and purely geometric transition which occurs when a given packing of particles reaches the maximum compression state above which particles start to overlap. More recently, the observation of remarkable scaling properties on the approach to jamming led to the conjecture that this zero temperature "critical point" could determine the properties of dense particle systems within a region of the parameter space to be determined, which in principle could include thermal and stressed systems. Fifteen years of intense theoretical and experimental work later, what have we learned about Jamming and glassy dynamics ? In this paper, we discuss these issues in the light of the experiments we have been conducting with vibrated grains.

Keywords: Granular media, Jamming, Glasses
PACS: Granular models of complex systems. Compaction, granular systems. Critical points, dynamic critical behavior.

INTRODUCTION

In a loose sense, Jamming describes all the situations where an assembly of particles gets stuck in a disordered configuration and stops flowing, ranging for instance from silo clogging to traffic jams. In the late 90's, the Jamming paradigm – *i.e.* a unified description of the onset of mechanical stability in divided matter – emerged to encompass in an unique framework these phenomena [1]. The "Jamming diagram" [2] illustrates this idea in the form of a Temperature-Density-Stress phase diagram of Jamming. This challenging proposal has been the starting point for a fantastic number of theoretical and experimental studies [3].

From a theoretical point of view, the simplest case of athermal and frictionless soft spheres packings has been extensively studied [4, 5, 6, 7] and now serves as a reference situation for which Jamming has a precise meaning: the transition occurs when the system can not be compressed further without allowing overlaps between particles. From that point of view, it is essentially a matter of satisfying geometric constraints, and indeed, a formal identification with algorithmic has been established [8, 9]. For athermal systems the Jamming transition is intrinsically out-of-equilibrium, which requires to state precisely the protocol used to prepare the system. Yet, many features of the transition appear to be protocol independent [10] and for a given protocol on an infinite system, the Jamming transition is entirely controlled by the packing fraction. The transition occurs at the so-called "point J" and coincides with the onset of isostaticity [11], *i.e.* the number of sterical and mechanical constraints imposed at the contacts matches exactly the number of degrees of freedom describing the particles. A number of geometrical and mechanical quantities exhibit clear scaling laws with the distance to jamming [3]. One prominent signature of jamming is the singular behavior of the average number of contacts per particle $z - z_J \propto (\phi - \phi_J)^\alpha$, where z_J is equal to 2 times d, the space dimension, ϕ_J is the packing fraction at point J, and $\alpha \simeq 0.5$ [4, 12]. The distribution of the gaps between particles displays a delta at zero and a square root decay for increasing gaps, which is the key to the singular behavior of the average contact number [7, 13, 14, 15].

From a practical point of view, real systems always include more complicated interactions such as friction for dry grains or hydrodynamics interactions for suspensions or foams. It is not clear *a priori* that one can safely neglect them. Still, careful experiments with photoelastic grains [12], emulsions [16, 17] and foams [18] have demonstrated the relevance of point J to describe their mechanical properties.

In addition, real systems that jam or unjam usually undergo micro or macroscopic motion: either the particles are small enough to be thermally agitated (*e.g.* colloidal suspensions, micro-emulsions) or some external forcing triggers mechanical vibrations (*e.g.* vibrated granular media, granular flows). A natural way to investigate

Powders and Grains 2013
AIP Conf. Proc. 1542, 25-31 (2013); doi: 10.1063/1.4811862

the effect of dynamics close to point J is to re-consider the case of soft spheres, but now in the presence of thermal fluctuations [19]. In principle, this allows one to use modern tools of equilibrium statistical physics. However, one soon realizes that for the packing fractions of interest, the system gets naturally dynamically arrested in non-equilibrium glassy states. Hence, describing thermal soft spheres in the vicinity of point J requires first to handle the complexity of the glass state, a notoriously difficult task. Within some approximations, this has been achieved only recently for both soft spheres [6, 7] and hard spheres [14, 20, 21]. This description recovers all the observed scalings in temperature and packing fraction *but* the square root singularity of the pair correlation function when $T = 0^+$ and $\phi = \phi_J^+$. This discrepancy, together with the onset of a diverging length in the vibrational properties of the jammed state [22], suggest that larger scale correlations must be taken into account.

Finally, the steep increase of the relaxation times associated with glassy behavior seriously hampers experimental work [23, 24, 25, 26]: samples brought to the high packing fractions of Jamming are deep into the glass phase and are difficult to manipulate on reasonable timescales. This difficulty can be dodged using p–NIPAM micro-gel particles, which can be inflated by slightly decreasing the temperature around the ambient. Using this trick, one can flow the sample into the observation cell and then increase the packing fraction [27, 28]. Furthermore, choosing the range of particle size and softness, one can in principle tune the relative importance of Brownian motion as well as the ratio of the thermal to the elastic energies when particles overlap. However the intrinsic difficulty remains: the time scales for equilibration in a given metastable state become prohibitively long as soon as one tries to approach the $T = 0^+$ limit. For athermal granular media, the situation is similar: they need some mechanical energy to be maintained in a non-equilibrium steady-state (NESS). As for thermal systems, this requires extremely slow compaction of the sample in order to avoid aging dynamics on the experimental timescales [29, 30]. For that reason, most granular experiments actually probe the glass transition and not the Jamming one [31, 32, 33].

In the following, we shall recast several experimental results to illustrate the above considerations. In the first section, we describe the microscopic mechanisms at play in granular systems approaching the glass transition and emphasize the decreasing role of facilitation associated to the emergence of large-scale dynamical heterogeneities [34, 35, 36]. In the second section, we experimentally study the vicinity of the Jamming transition by investigating both statics and dynamics of the contact network in a horizontally shaken bi-disperse packing of brass or photo-elastic discs. This packing was first prepared in a granular glass state, namely a frozen structure of vibrating grains, by very slow compression while maintaining a mechanical excitation [37, 38]. We conclude by comparing our observations with numerical simulations of thermal frictionless soft spheres [19].

SPATIO-TEMPORAL ORGANIZATION OF THE RELAXATION CLOSE TO THE GLASS TRANSITION

In this section, we provide an overview of the mechanisms at play during the appearance of large dynamical heterogeneities close to the characteristic dynamical arrest associated with the glass transition. Let us start at the microscopic level and follow one single particle: a typical trajectory $r_p(t)$ is shown on figure 1-left. The particle performs localized, vibrational motion around a metastable position, as in a disordered solid, forming "cages" that are interrupted by rapid excursions called "cage jumps". Jumps are by definition irreversible, which distinguishes them from ratling movements. The jump lengths distribution is bell-shaped with a well-defined average value, which is only a small fraction of the particle size. This suggests that jumping movements come from *cooperative* events involving a potentially large number of particles moving by a small amount. This observation is at the root of the idea of cooperative motion and dynamical heterogeneities.

This immediately translates into the statistics of motion: the displacement distributions along an arbitrary direction are composed of a central Gaussian part, corresponding to the short time vibration, and large exponential tails associated with the rare jumping events. It is remarkable that these distributions have the same structure over a broad lag time window, comprising the structural relaxation. The width of these distributions also reflects the existence of the cages: the mean square displacements exhibit a sub-diffusive plateau at intermediate timescales [32]. Then, to quantify the relaxation of the density field, one introduces:

$$Q_{p,t}(\tau) = exp\left(-\frac{||\Delta\vec{r}_p(t,t+\tau)||^2}{2\sigma(\tau)^2}\right), \qquad (1)$$

where $\Delta\vec{r}_p(t,t+\tau) = \vec{r}_p(t+\tau) - \vec{r}_p(t)$ is the displacement of the particle p, between t and $t+\tau$ and $\sigma(\tau)^2 = \left\langle ||\Delta\vec{r}_p(t,t+\tau)||^2 \right\rangle$ is the root mean square displacement on a lag τ. The interpretation is straightforward: when a particle p moves less (resp. more) than $\sigma(\tau)$ between t and $t+\tau$, $Q_{p,t}(\tau)$ remains close to one (resp. decreases to zero). Averaging this quantity over all particles, one obtains $Q_t(\tau) = \left\langle Q_{p,t}(\tau) \right\rangle_p$, which evaluates the overall relaxation of the system between t and $t+\tau$. Typically the relaxation time τ_α is then given by $\langle Q_t(\tau_\alpha)\rangle_t = 1/2$. $Q_t(\tau)$ is a highly fluctuating quantity, the fluctuations of

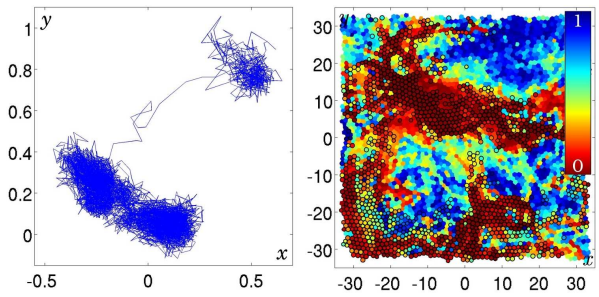

FIGURE 1. Left: Typical trajectory, composed of several cage jumps. The experimental setup is a bi-dimensional fluidized bed of beads, the motion of which is excited by an upward flow of air [32, 39]. Space units are in particle diameter. Right: Spatial field of the local relaxation $Q_{p,t}(\tau^*)$. Particles jumping between t and $t+\tau^*$ are represented with black circles, and lye preferentially in the moving areas. From [35].

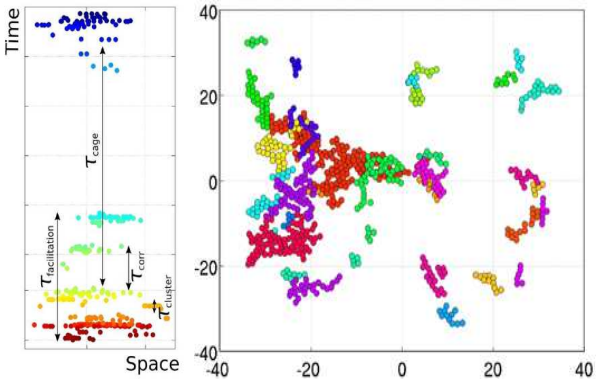

FIGURE 2. Left: Sketch of the spatio-temporal organization of the cage jumps in a given region of space. Right: Spatial location of cage jumps, showing how they facilitate each other to form dynamical heterogeneities. From [35].

which betray the heterogeneous character of the dynamics, in a way analogous to the way fluctuations of magnetization indicate the proximity of the para-ferro magnetic transition. However, in the present case, such fluctuations depend on the timescale τ on which the relaxation is evaluated, hence the name of *dynamical heterogeneities*. These fluctuations are maximal for a given τ^* of the same order as τ_α.

Dynamical heterogeneities are a key characteristic of glassy dynamics [40]. They were first proposed to explain the stretched exponential relaxation of supercooled liquids. At low enough temperature or high enough packing fraction, the dynamics becomes heterogeneous: domains of slow and fast relaxation coexist in real space and slowly evolve on long time scales. The length-scale associated with these heterogeneities suggests that the slowing down of the dynamics is related to a collective phenomenon, possibly to a true phase transition. Many different possible origins of these heterogeneities have been highlighted in the literature, *e.g.* dynamic facilitation [41], soft modes [42, 43], proximity to a mode coupling transition [44, 45] and growing amorphous order [46].

To gain insight on the microscopic origin of dynamical heterogeneities, efforts have been made to localize the cage jumps in space and time (see for instance the iterative algorithm introduced in [35]). Figure 1-right displays the spatial field of the local relaxation $Q_{p,t}(\tau^*)$ for a cyclic shear granular experiments [31, 35] with, superposed on top of it, the location of the cage jumps that have occurred between t and $t+\tau^*$. The distribution in space and time of these events is far from homogeneous, and the left panel of figure 2 illustrates the different timescales involved during the relaxation process: first, cage jumps form clusters in space which occur on a relatively short time scale $\tau_{cluster}$. The distribution of the lag times separating two adjacent clusters can be described by the superposition of two distributions: one for the long times corresponding to the distribution of the time spent by the particles in its cage τ_{cage}, and one for the short delays between adjacent clusters τ_{corr}. When the ratio of these two timescales is large enough, the clusters form well separated avalanches, whose spatial organization is illustrated in the right panel of figure 2. One can see how the clusters spread and build up a uncorrelated region. This mechanism is a perfect illustration of facilitation: a local relaxation has a very high probability of happening nearby another relaxation after a certain time, which is short compared to the macroscopic relaxation time but large compared to the microscopic one. In the present case, the avalanches have a finite duration: they *are* the dynamical heterogeneities.

This scenario depends on the distance to the glass transition. Let us illustrate this in the case of the fluidized bed experiment described in [39, 47]. The spatio-temporal facilitation patterns are represented on figure 3 for three packing fractions, the time axis being rescaled with respect to the relaxation time τ_α. We draw all cage jumps (black dots) and link the ones separated by a lag time less than τ_{corr}. This defines a network whose vertices are the cage jumps and whose edges are the orientated links towards facilitated jumps. For the loosest packing fraction, all jumps are connected with facilitation links and form a highly interconnected monolith. Dynamical facilitation is thus conserved on timescales relevant for structural relaxation. When raising the packing fraction, well-defined avalanches emerge. Several independent avalanches start and end within a time interval of the order of the relaxation timescale and dynamical facilitation is clearly not conserved anymore. The above observations suggest that at even higher density each avalanche would reduce to a single cluster and that dynamical facilitation would dis-

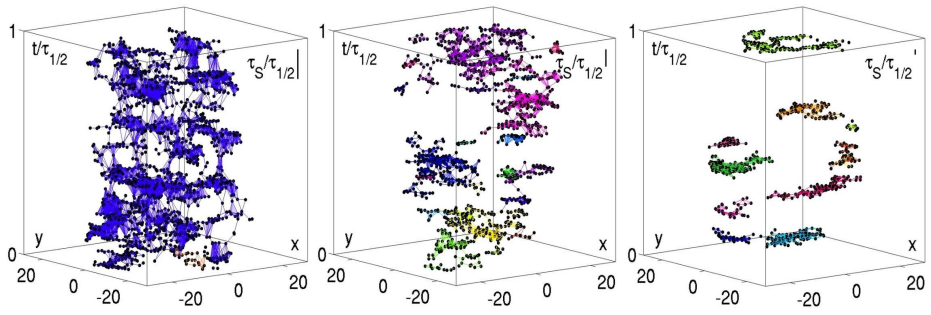

FIGURE 3. Facilitation patterns in space and time during the typical relaxation time $\tau_{1/2}(\phi) = \tau_\alpha(\phi)$ for 3 packing fractions : from left to right $\phi = 0.780,\ 0.791,\ 0.802$. The two directions of space are in the horizontal plane and time is the vertical axis. The ratio $\tau_S/\tau_{1/2}$ is given in the upper-right corners. Jumps are represented with black dots, and all possible tetrahedrons which edges are the facilitating links between jumps are shown, forming volumes. Each separate connected structure has a different color. From [36].

appear completely.

To check that the above characterization of dynamical heterogeneities is not restricted to granular packings, we have performed the same analysis with simulated data of a supercooled liquid at equilibrium, namely a bidimensional binary mixture of $N = 5,760$ particles enclosed in a square box with periodic boundary conditions, interacting via purely repulsive non-additive potentials of the form $u_{ab}(r) = \varepsilon(\sigma_{ab}/r)^{12}$. Once the timescales are properly rescaled, the similarities with the granular media experiments are astonishing [34, 48].

DYNAMICAL AND STRUCTURAL CROSSOVER IN THE VICINITY OF THE JAMMING TRANSITION

We now come to the description of a granular system which is brought to even higher packing fractions; its structure is thus *totally* frozen. To obtain these dense packings, the system has been prepared through a slow compression protocol in the presence of vibrations [37]. The main difference with the preceeding section is that the grains are free to vibrate in this frozen structure but they can not escape their cage, at least on the experimental timescales. In this case, the most interesting part of the dynamics lies in the contact network; it is naturally quantified by an estimator for the relaxation of the contact network between t and $t+\tau$, similar to the one introduced above to quantify the density relaxation:

$$Q^z(t,\tau) = \frac{1}{N}\sum_i Q_p^z(t,\tau), \qquad (2)$$

where $Q_p^z(t,\tau) = \Theta(2 - |\delta z_p(t,\tau)|)$, with $\Theta(.)$ the Heavyside function and $\delta z_p(t,\tau)$, the change in number of contacts of grain p between t and $t+\tau$. Figure 4-left displays $Q_z(\tau) = \langle Q^z(t,\tau)\rangle_t$ for various packing fractions, where$\langle . \rangle_t$ denotes the time average. For the largest packing fractions, $Q^z(\tau)$ remains constant at values above 0.93, indicating the absence of long-time decorrelation of the contact network: once formed, the contacts are established permanently. The sole decorrelation occurs at very short times scales and comes from the fast ratling dynamics of a minority of grains. For lower packing fractions, long time relaxation sets in and contacts rearrange. These two distinct behaviors allow us to define a crossover packing fraction $\phi^\dagger$. It is indicated with a black dashed line on the right panel of figure 4. This crossover also separates two different regimes in the dependence of the average number of contact with the packing fraction (see fig 4-right): below $\phi^\dagger$, the average number of contact z is roughly constant, whereas it steeply increases above $\phi^\dagger$.

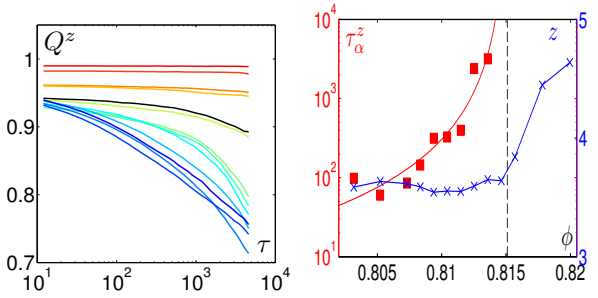

FIGURE 4. Structural crossover at the contacts. Left: Structure factor of the neighborhood links Q^z as a function of the lag time τ. Color code spans from blue (low packing fractions) to red (high packing fractions). The black line indicates the crossover packing fraction $\phi^\dagger$. Right: Relaxation time of the contact network, τ_α^z (■, left axis), and average contact number z (×, right axis) as functions of the packing fraction ϕ. The plain red line is a fit of the form $\tau_\alpha^z \sim (\phi_J - \phi)^{-2.0}$. The dashed line indicates $\phi^\dagger = 0.8151$. From [38].

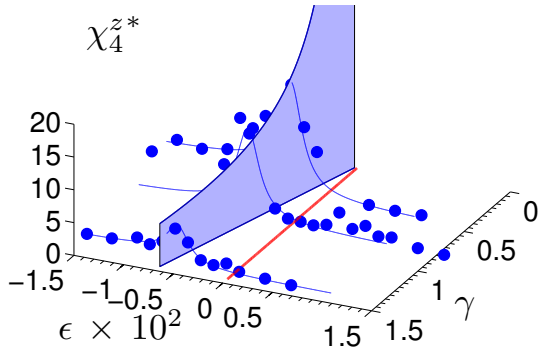

FIGURE 5. Maximal dynamic susceptibility of the contacts χ_4^{z*} as a function of the reduced packing fraction ε and the reduced vibration magnitude γ.

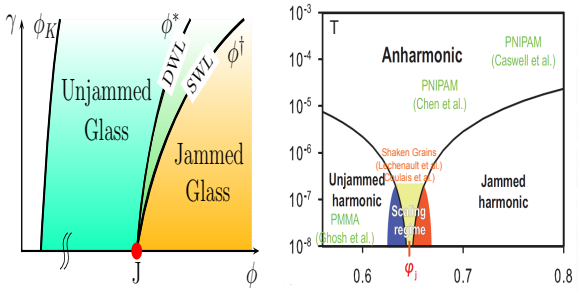

FIGURE 6. Phase Diagram. Left: Sketch summarizing our observations; $\phi_K(\gamma)$ is the expected glass transition, $\phi^*(\gamma)$ and $\phi^\dagger(\gamma)$ are respectively the dynamical and the structural crossover lines merging at point J. Right: Location in the parameter space of some of the existing colloidal experiments and the present vibrated granular one (adapted from [19])

Interestingly, the dynamics of the contact network below $\phi^\dagger$ exhibits strong fluctuations and dynamical heterogeneities, albeit of a different kind from the one described in the previous section. Here the heterogeneities are relative to the degrees of freedom describing the contacts, not the position of the grains. To quantify such heterogeneities, one can compute the dynamical susceptibility (see [40]) which estimates the range of spatial correlations in the dynamics of the contact network:

$$\chi_4^z(\tau) = N \frac{Var(Q^z(t,\tau))}{\langle Var(Q_p^z(t,\tau))\rangle_p}, \qquad (3)$$

where $Var(.)$ denotes the variances sampled over time and $\langle . \rangle_p$ denotes the average over the grains.

We have studied how the maximum χ_4^{z*} of $\chi_4^z(\tau)$ depends on both the reduced packing fraction $\varepsilon = (\phi - \phi^\dagger)/\phi^\dagger$ and the reduced vibration frequency $\gamma = (f - f_0)/f_0$, where f_0 is the minimal frequency requested to inject energy into the packing (see figure 5). χ_4^{z*} is non-monotonic with respect to the reduced packing fraction, and has a maximum value at a negative reduced packing fraction ε^*. This points out the existence of a dynamical crossover corresponding to a maximally collective relaxation of the contact network at a packing fraction *lower* than the structural crossover. Besides, when γ is decreased one observes that (*i*) ε^* vanishes, *i.e.* the location of the dynamical crossover moves towards $\phi^\dagger$, and (*ii*) the magnitude of the maximum χ_4^{z*} significantly increases as $1/\gamma$. Hence, we can safely conjecture that in the limit of no effective mechanical excitation the structural and dynamical crossovers merge, while the length scale associated with the dynamical crossover diverges. This strongly suggests, as sketched on figure (6)-left, that we have indeed probed the vicinity of a critical point, which in the present case ought to be the Jamming transition at zero temperature.

However, as already stated, the present granular system unlike thermal systems is in an out-of-equilibrium and mechanically driven state; and one must remain cautious when comparing with packings of thermal soft spheres. Recent numerical simulations [7, 19, 49, 50] suggest that the similarities with thermal systems are much stronger than one may have expected at first sight. For instance, the structural crossover reported here might be related to the finite temperature first-peak pair-correlation maxima near the Jamming point reported in [7, 28, 49]. More specifically, in [19] the authors report an extensive study of the dynamics close to point J in the temperature-density parameter space, which they conclude by comparing with existing colloidal experiments. To do so, they essentially use the Debye-Waller factor, namely the size of the cage surrounding the particles, as a sensitive thermometer. They conclude that existing experiments with colloids are outside the scaling regime of point J, which extends only to very small temperature. In the present case, we can follow the same procedure to evaluate the kinetic energy in our system and situate our experiments with respect to point J. According to their result, the experiment described here, as well as those performed with much harder grains [37, 51] are in a good position to have probed the dynamical criticality related to the jamming transition (see figure (6)-right).

DISCUSSION AND PERSPECTIVES

We have investigated dense, driven granular assemblies in the vicinity of the Glass and the Jamming transitions in various experimental setups. This work demonstrates that the experimental challenges one could *a priori* expect to face with these far-from-equilibrium systems can be overcome. Furthermore, the macroscopic particles can be individually tracked and the contact network can be

inferred, which broadens the range of accessible time and length scales.

Our study of the dynamics close to the glass transition has revealed the role of the cage jumps as the elementary events of relaxations. Then, by a careful examination of the spatial and temporal correlations, we could relate the large space and time scales dynamical properties of the system to that of these localized and quasi instantaneous excitations. This has shed new light on the role of facilitation, when approaching the glass transition. A first comparison with a model glass former shows strong similarities. Work under progress will tell us whether the above conclusion applies to this thermal system.

The examination of the contacts dynamics in the glass phase has allowed us to identify two crossovers, one structural and one dynamical. When the mechanical excitation is reduced towards zero, the two crossovers merge, while the length scale associated with the dynamical crossover sharply increases. This is an important experimental result which supports the critical nature of the zero temperature point J. Again, comparison with thermal soft spheres are encouraging and tell us that the simplest thermal model are relevant to describe a rather large class of systems.

Yet, the microscopic details of each specific system will come into play at some point. For instance, in the experiments conducted with the photo-elastic discs, the friction coefficient amongst the grains is typically $\mu = 0.7$ and the careful reader will have noticed that the jamming packing fractions reported here have a lower value than those obtained for frictionless particles. Still our results demonstrate that in the dynamical regimes probed by our experiments, friction does not seem to be a qualitatively relevant parameter. Understanding whether it impacts the quantitative scaling properties close to point J requires further studies, presumably numerical ones. In addition, those who have performed experiment with shaken grains know that convection eventually always sets in, whatever the care taken to avoid it. Such convection is a low frequency mode by which NESS dissipate energy and which is usually filtered out from the data. Whether it interacts with the other modes of the dynamics is an interesting open issue.

Finally, we have recently studied vibrated granular media, albeit of a new kind: each grain is a disc with a built in polar asymmetry, which enables them to move quasi-balistically on a large persistence length [52, 53]. Alignment occurs during collisions as a result of self-propulsion and hard core repulsion. Varying the amplitude of the vibration, we have observed the onset of large-scale collective motion and the existence of giant number fluctuations. This experimental system is a realization of what is now called active matter, a fascinating new emerging field of soft matter physics. Investigating how such systems behave at large packing fractions, when steric constraints comes into play and slow down the dynamics, has only just started to be investigated [54] and will certainly attract a lot of attention in the near future. For instance, one may simply wonder whether the glass phase survive in such active systems.

ACKNOWLEDGMENTS

The content of this paper owes a lot to our collaborators, without whom none of the present ideas and results would have been developed: G. Marty, F. Lechenault, B. Behringer, G. Biroli, L. Berthier and J.-P. Bouchaud. Several papers written with them have inspired the present notes. Let me also thank Cécile Wiertel-Gasquet and Vincent Padilla, who turned our dreams into real experiments. We also want to thank A. Abate, D. Durian, A. Widmer-Cooper and P. Harrowell for having shared data with us.

REFERENCES

1. M. E. Cates, J. P. Wittmer, J.-P. Bouchaud, and P. Claudin, *Phys. Rev. Lett.* **81**, 1841–1844 (1998).
2. A. J. Liu, and S. R. Nagel, *Nature* **396**, 21–22 (1998).
3. M. van Hecke, *Journal of Physics: Condensed Matter* **22**, 033101 (2010).
4. C. S. O'Hern, S. A. Langer, A. J. Liu, and S. R. Nagel., *Phys. Rev. Lett.* **88**, 075507 (2002).
5. C. S. O'Hern, L. E. Silbert, A. J. Liu, and S. R. Nagel, *Phys. Rev. E* **68**, 011306 (2003).
6. L. Berthier, H. Jacquin, and F. Zamponi, *Phys. Rev. E* **84**, 051103 (2011).
7. H. Jacquin, L. Berthier, and F. Zamponi, *Phys. Rev. Lett.* **106**, 135702 (2011).
8. F. Krzakala, and J. Kurchan, *Phys. Rev. E* **76**, 021122 (2007).
9. F. Krzakala, A. Montanari, F. Ricci-Tersenghi, G. Semerjian, and L. Zdeborová, *Proceedings of the National Academy of Sciences* **104**, 10318–10323 (2007).
10. P. Chaudhuri, L. Berthier, and S. Sastry, *Phys. Rev. Lett.* **104**, 165701 (2010).
11. A. V. Tkachenko, and T. A. Witten, *Phys. Rev. E* **60**, 687–696 (1999).
12. T. S. Majmudar, M. Sperl, S. Luding, and R. P. Behringer, *Phys. Rev. Lett.* **98**, 058001 (2007).
13. L. E. Silbert, D. Ertaş, G. S. Grest, T. C. Halsey, and D. Levine, *Phys. Rev. E* **65**, 031304 (2002).
14. G. Parisi, and F. Zamponi, *Rev. Mod. Phys.* **82**, 789–845 (2010).
15. A. Donev, S. Torquato, and F. H. Stillinger, *Phys. Rev. E* **71**, 011105 (2005).
16. I. Jorjadze, L.-L. Pontani, K. A. Newhall, and J. Brujić, *Proceedings of the National Academy of Sciences* **108**, 4286–4291 (2011).
17. J. Brujic, C. Song, P. Wang, C. Briscoe, G. Marty, and H. A. Makse, *Phys. Rev. Lett.* **98**, 248001 (2007).
18. G. Katgert, and M. van Hecke, *EPL (Europhysics Letters)* **92**, 34002 (2010).

19. A. Ikeda, L. Berthier, and G. Biroli (2012).
20. M. Mézard, and G. Parisi, *The Journal of Chemical Physics* **111**, 1076–1095 (1999).
21. H. Yoshino, and M. Mézard, *Phys. Rev. Lett.* **105**, 015504 (2010).
22. M. Wyart, S. R. Nagel, and T. A. Witten, *EPL (Europhysics Letters)* **72**, 486 (2005).
23. P. Pusey, and W. van Megen, *Nature* **320**, 340 (1986).
24. P. N. Pusey, and W. van Megen, *Phys. Rev. Lett.* **59**, 2083–2086 (1987).
25. W. van Megen, and S. M. Underwood, *Phys. Rev. E* **49**, 4206–4220 (1994).
26. G. Brambilla, D. El Masri, M. Pierno, L. Berthier, L. Cipelletti, G. Petekidis, and A. B. Schofield, *Phys. Rev. Lett.* **102**, 085703 (2009).
27. K. N. Nordstrom, E. Verneuil, P. E. Arratia, A. Basu, Z. Zhang, A. G. Yodh, J. P. Gollub, and D. J. Durian, *Phys. Rev. Lett.* **105**, 175701 (2010).
28. Z. Zhang, N. Xu, D. T. N. Chen, P. Yunker, A. M. Alsayed, K. B. Aptowicz, P. Habdas, A. J. Liu, S. R. Nagel, and A. G. Yodh, *Nature* **459**, 230–233 (2009).
29. J. B. Knight, C. G. Fandrich, C. N. Lau, H. M. Jaeger, and S. R. Nagel, *Phys. Rev. E* **51**, 3957–3963 (1995).
30. P. Richard, M. Nicodemi, R. Delannay, P. Ribiere, and D. Bideau, *Nat Mater* **4**, 121–128 (2005).
31. G. Marty, and O. Dauchot, *Phys. Rev. Lett.* **94** (2005).
32. A. R. Abate, and D. J. Durian, *Phys. Rev. E* **74**, 031308 (2006).
33. K. Watanabe, and H. Tanaka, *Phys. Rev. Lett.* **100**, 158002 (2008).
34. R. Candelier, A. Widmer-Cooper, J. K. Kummerfeld, O. Dauchot, G. Biroli, P. Harrowell, and D. Reichman, *Phys. Rev. Lett.* **105**, 135702 (2010).
35. R. Candelier, O. Dauchot, and G. Biroli, *Phys. Rev. Lett.* **102** (2009).
36. R. Candelier, O. Dauchot, and G. Biroli, *EPL (Europhysics Letters)* **92**, 24003 (2010).
37. F. Lechenault, O. Dauchot, G. Biroli, and J. P. Bouchaud, *EPL (Europhysics Letters)* **83**, 46003 (2008).
38. C. Coulais, R. P. Behringer, and O. Dauchot, *Eur. Phys. Lett.* **100**, 44005 (2012).
39. A. S. Keys, A. R. Abate, S. C. Glotzer, and D. J. Durian, *Nat Phys* **3**, 260–264 (2007), ISSN 1745-2473.
40. L. Berthier, G. Biroli, J.-P. Bouchaud, L. Cipelletti, and W. V. Saarloos, editors, *Dynamical Heterogeneities in Glasses, Colloids, and Granular Media*, Oxford University Press, 2011.
41. J. P. Garrahan, and D. Chandler, *PRL* **89**, 035704 (2002).
42. C. Brito, and M. Wyart, *J. Stat. Mech.* **8**, L08003 (2007).
43. A. Widmer-Cooper, H. Perry, P. Harrowell, and D. R. Reichman, *Nature Physics* **4**, 711–715 (2008).
44. C. Donati, S. Franz, S. C. Glotzer, and G. Parisi, *Journal of non-crystalline solids* **307**, 215–224 (2002).
45. G. Biroli, and J.-P. Bouchaud, *Europhys. Lett.* **67**, 21–27 (2004).
46. G. Biroli, J.-P. Bouchaud, A. Cavagna, T. Grigera, and P. Verrocchio, *Nature Physics* **4**, 771–775 (2008).
47. A. R. Abate, and D. Durian, *Phys. Rev. E* **74**, 031308 (2006).
48. G. Biroli, *Poincaré seminars* **XIII**, 37–67 (2009).
49. L. Wang, and N. Xu, *ArXiv e-prints* (2011).
50. M. Otsuki, and H. Hayakawa, *Phys. Rev. E* **86**, 031505 (2012).
51. F. Lechenault, O. Dauchot, G. Biroli, and J. P. Bouchaud, *EPL (Europhysics Letters)* **83**, 46002 (2008).
52. J. Deseigne, S. Leonard, O. Dauchot, and H. Chate, *Soft Matter* **8**, 5629–5639 (2012).
53. J. Deseigne, O. Dauchot, and H. Chaté, *Phys. Rev. Lett.* **105**, 098001 (2010).
54. S. Henkes, Y. Fily, and M. C. Marchetti, *Phys. Rev. E* **84**, 040301 (2011).